www.rericjournal.ait.ac.th

# Modelling, Simulation, and Enhancement of Hybrid Renewable Energy Systems for Purification Utilization

Mochammad Junus*, +, 1, Marjono#, Aulanni'am#, and Slamet Wahyudi$

**ARTICLE INFO**

*Article history:*
Received 27 April 2022
Received in revised form
07 September 2022
Accepted 11 November 2022

*Keywords:*
Hybrid energy
Off-grid
Optimization
Purification
Reverse osmosis

**ABSTRACT**

*The primary challenge in designing and executing purification plants is energy; this worry is magnified in isolated places with little or no connection to the primary power grid. This research evaluates a reverse osmosis filtration plant's off-grid hybrid alternative energy source. The facility, which has a purification capacity of 10 $m^3$, is located in the Malang district in Indonesia's western region. The site's climatic characteristics, such as air temperature, wind speed, solar irradiance, and clearness index, are obtained for better evaluation. The simulation was carried out using Homer software, and all potential PV/wind turbine/generator/battery combinations were computed and contrasted. Finally, the results of two different strategies, a fully renewable hybrid energy system with and without a backup generator, are shown. Experiments have shown an off-grid hybrid energy source consisting of a 12.5 kW PV panel with a power output of 335 W and an array of batteries totaling 205 Ah. A backup generator is the most cost-effective option. It costs $0.37 to produce one unit of energy; however, the cost of each unit of energy produced by an integrated PV/wind turbine/battery system is $0.275.*

## 1. INTRODUCTION

Access to sufficient freshwater is a prerequisite for sustainable development, yet salinity renders around 98 percent of available water unusable [1]. Many nations worldwide face a water crisis exacerbated by climate change and population increase [2]. The Middle East, a semi-arid and desert area, is particularly hard hit by this problem [3]. This region's physical water risk index is high (Figure 1) [4]. For example, the annual precipitation in Indonesia is less than 130 mm (Figure 2), which is insufficient for homes.

Purification appears to be the only solution in many circumstances. Nowadays, industrial purification uses reverse osmosis with multi-stage flashing (MSF). MSF is a thermal approach that is dependable and well-developed, but requires more energy [5]. Alternatively, RO membrane implementation is more difficult and requires pre-treatment, but it consumes less energy and produces less pollutants. A RO plant consists mostly of six components. (Figure 3). Due to the characteristics of membranes (water-repellent, mass-transfer-resistive-low, high-temperature-stable, and chemical-resistant; especially useful against acids and bases), a pre-treatment process, including initial filtration, acid addition, and coagulation, is required in industrial desalination plants. There is risk of membrane damage or decreased plant yield without a pre-treatment step [6]. Depending on the needs of the end-user, the post-treatment procedure can vary from plant to plant (*e.g.* advanced oxidation for achieve high water recovery) [7].

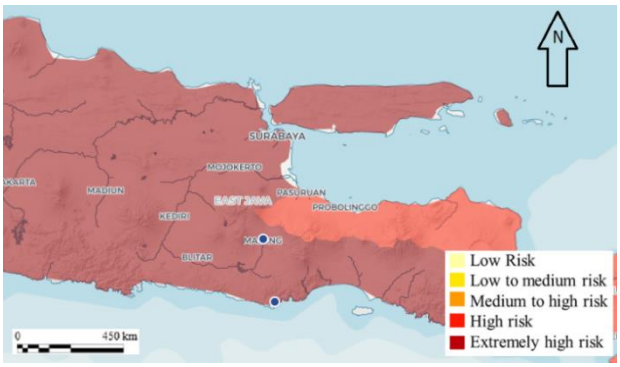


**Fig. 1. Physical threat to Malang's water supply.**

A semi-permeable membrane is one of the numerous membrane types utilized in the RO process. RO purification uses a semi-permeable membrane that only enables water to pass through. The most prevalent reverse osmosis membranes are cellulose acetate (CA) and thin film composite membranes (TFC). Membrane research dominates the literature. The current study improved the quality of porous materials [8], [9] and

*Brawijaya University, Mayjen Haryono 169, Malang 65145, Indonesia.

+ Department of Electrical Engineering, State Polytechnic of Malang, Soekarno Hatta 9, Malang 65141, Indonesia.

# Faculty of Mathematics and Natural Sciences, Brawijaya University, Malang 65145, Indonesia.

$ Faculty of Engineering, Brawijaya University, Malang 65145, Indonesia.

1Corresponding author:
Email: mochmmad.junus@polinema.ac.id.

membrane structure [10] to improve the RO filtering rate.

Oxygen plasma was employed to create nanoporous single-layer graphene for purifying purposes, according to Surwade and colleagues [11]. Some even attempted using novel materials in membranes to improve their characteristics [11], [12]. Kalankesh *et al.* presented a microbial purification cell that might create power while purifying water; Rajinder reduced electricity usage by 18% by heating his dual-purpose membrane [10].

Despite all the attempts to improve filtering efficiency, the RO system still needs a high-pressure environment to create osmosis pressure and enable fresh water to pass through membrane pores. Membrane type, plant design, and even water salinity can influence the necessary pressure or energy. For example, an increase in feed water salt concentration from 1,500 to 4,500 ppm can boost energy production by as much as 60% [13]. The high-pressure pumping step, which accounts for around 85 percent of the system's overall energy consumption, is the most energy-intensive part of the purifying process [14].

Among the most significant issues facing purifying systems nowadays are the high price of electricity, the difficulty in acquiring energy in remote areas, and the terrible environmental consequences of the gases produced by conventional fuels and other energy sources. As part of their attempts to attain near-zero net pollutant removal rates, researchers have examined the usage of new sustainable resources in plants [15]–[17]. Non-renewable energy sources pose a serious dilemma, as they are derived from natural processes that require millions of years to complete, as proven by much research on the deployment of solar energy and photothermal energy [18], wind energy [19], [20], and a variety of other ways [21]. Solar and wind power are used in just 1% of all modern purification plants, even though they appear to be an attractive alternative to fossil fuels [22]. Renewable energy sources cannot be used as a stand-alone system because of their stochastic nature and intermittent energy supply [23]. The system will remain entirely powerless for several days if the weather is gloomy and there is no breeze. In this case, hybrid renewable energy sources might provide a viable answer. Combining two or more energy sources can result in a hybrid energy system that can provide all or a portion of the power expended by a customer (Figure 4).

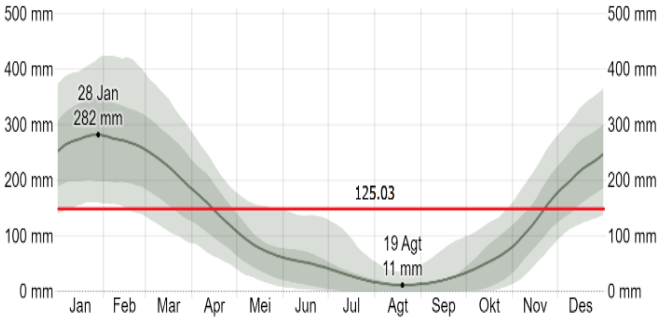


**Fig. 2. Annual rainfall in Malang.**


**Fig. 3. The significant components of a reverse osmosis plant**

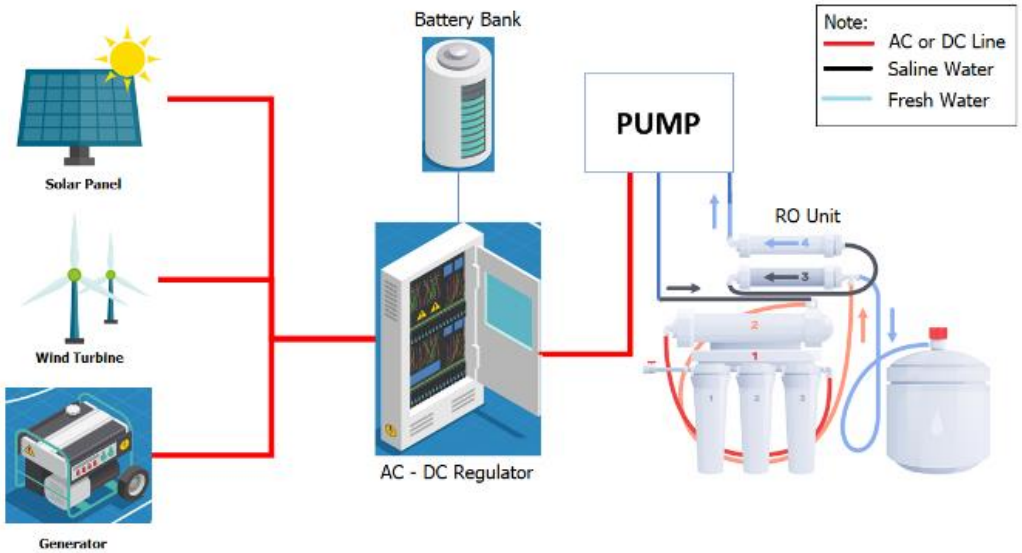


**Fig. 4. A diagrammatic representation of a hybrid energy system for a RO plant.**

The hybrid system has all the benefits of a single green energy source, but it is also more efficient and can produce energy through a more equitable exchange. Like other renewable systems, this system may be created in distant regions without access to power grids, but it is expensive and challenging to execute. Extending the use of hybrid energy systems to include more equipment increases running and maintenance expenses while complicating the system's operation and maintenance. Managing the output power of each generator, which may be alternating current or direct current, in a hybrid system necessitates the use of a converter and a control system. Overall, with careful analysis and optimization, a desalination plant can be powered by a hybrid energy system as depicted in Figure 5, which reduces operating costs while producing fewer greenhouse gases.

A choice is made based on each component's priority and size in the optimization process. This is associated with the required power load, the power output of each energy source, the cost of each component, the payback period, and the operating costs. Therefore, it is necessary to evaluate each component's size as part of the optimization process, and then the choice will be made under the priorities established for each component [24]. Many methodologies have been developed to determine the optimal energy mix from renewable sources [25]–[27]. Some studies used commercially available software, such as iHOGA, RETScreen, HYBRID, and other similar programs [27]–[29]. In addition, the researchers tested a model based on optimization techniques such as the genetic algorithm, bee swarm algorithm, and the search method [2], [3], [30]–[32].

With encouraging results, several energy sources and consumers were simulated and optimized using Homer Pro (Homer). Any single or hybrid energy source can be used to create power in the simulated energy system. Batteries can be used when storing energy in a remote system, such as the purification plant depicted. The battery can significantly reduce the size and quantity of energy generators. For example, simulating a hybrid system for a purification plant may be done using Homer, which can also simulate the quantity of battery storage needed.

The first objective of this article is to examine the viability of employing renewable energy sources for a major power consumer, namely a desalination plant. The second objective is to determine the life cycle and costs of hybrid energy for such a consumer. To achieve sustainable development, a system with a long lifespan, low expenses, and high output is essential. This simulation enhances our understanding of the capital cost, net cost, maintenance cost, and operating cost (based on the types and number of pieces of equipment). In addition, a realistic simulation of the hybrid system can shed light on the environmental implications of such a system.

In this paper, the overall desalination potential of an off-grid hybrid renewable energy system is evaluated. In doing so, the meteorological features of the location are studied, and daily wind speed, sun radiation, clear index, and air temperature data are taken into account. Using Homer Pro software [33], the data is examined and all conceivable instances are considered separately. Later, a 20-year project lifespan is evaluated, and the net price of filtered water is compared with each feasible hybrid system configuration. Finally, the most optimal combination is offered, followed by a sensitivity analysis. Although the provided method of assessment can be employed in many places with varied energy sources, a dry region in the hamlet of Tambakrejo in western Indonesia's South Malang area was examined. This community is small and sparsely populated. For the freshwater demands of the residents, a grid-independent RO system may be utilized.

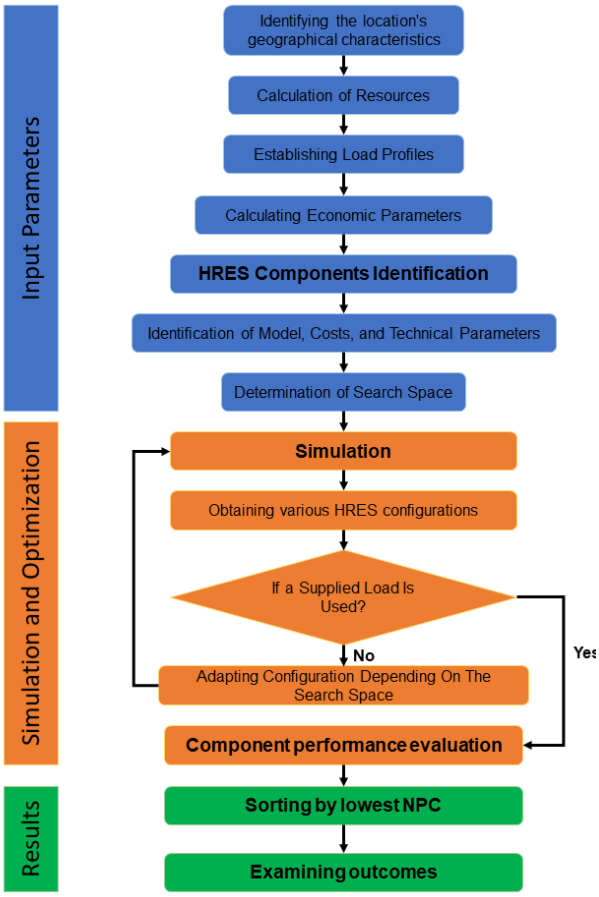


**Fig. 5. Diagram of the hybrid energy system troubleshooting procedure for the purification plant.**

## 2. MATERIALS AND METHODS

### *2.1 Load Profile*

A rough estimate of how much RO energy will be required is the first stage in the simulation. Purification rate (liters/hour) and energy consumption per liter are two separate problems for the RO system. To begin, although the typical individual in the world uses 200 liters of water per day, this figure is more significant in Indonesia. Tambakrejo's population of 100 persons uses 10,400 liters of water per day (10.4 $m^3$/day), which is 60 liters higher than the international limit. In a hybrid renewable energy system with varying energy capacity, it is vital to disperse water demand throughout the day. Daily, a single family's water consumption is shown in graph form in Figure 6 [34]. As seen in the graph, the

lowest water demand occurs between the hours of twelve and four a.m., while the most considerable demand occurs between seven and eight a.m.

Consider the amount of energy it takes to filter each liter of water using RO as a second consideration in the load profile. Figure 7 depicts the RO system that was employed in this study. A high-pressure Bertolini pump (type WBL 11xx) with a maximum pressure of 11,024 kPa at 151.84 rad/s is incorporated. The maximum flow rate of the pump is 10.991 l/min. The AC motor's voltage and current are monitored to determine how much power the RO consumes (Figure 8). South Malang Seawater has a total dissolved salts (TDS) value of 42.052 kg/L, resulting energy consumption. (Table 1) [35]. TDS concentration was maintained at 42 kg/liter, and the air temperature was maintained at room temperature for the test duration. The reverse osmosis system uses 5.8 kWh of electricity to desalinate 1 $m^3$ water. This is a large amount of energy compared to what RO plants typically generate (five kWh energy for purifying each $m^3$ of water) [36]. As a result, the hybrid system must contribute at least 60.3 kWh of energy per day to the RO system.

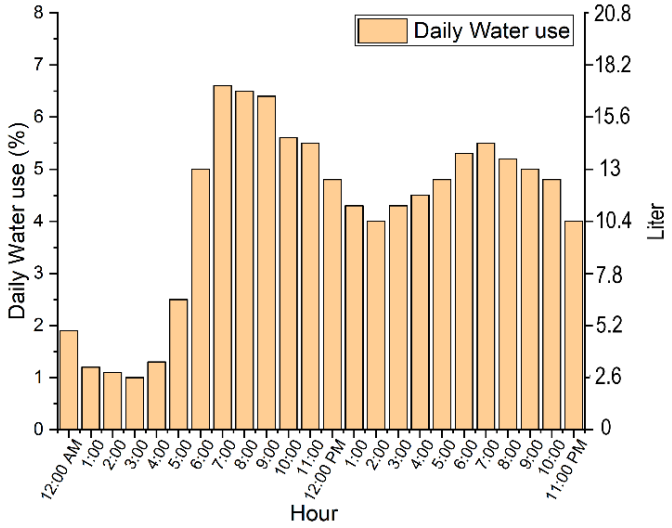


**Fig. 6 A single family's hourly freshwater demand.**

**Table 1. South Malang's seawater concentration.**

| Substance | Purity (mg/liter) |
|---|---|
| Calcium | 459 |
| Magnesium | 1,504 |
| Natrium | 12,802 |
| Kalium | 458 |
| $HCO_3$- | 164 |
| $S0_4$- | 3,141 |
| Cl- | 23,114 |
| TDS | 41,052 |
| Ca++ | 459 |

Abbreviation: TDS, total dissolved salts.

### *2.2 RO's Hybrid Power Sources*

The power generation system utilizes renewable and fossil fuel energy sources to provide a consumer with enough electricity. Simulating fuel-based energy is simple. Depending on fuel costs and availability, these projects can use a variety of generators. However, the potential of any renewable energy source varies depending on the area. A thorough grasp of critical aspects of generation power is required for a realistic simulation.

### *2.3 Solar Energy*

Due to Indonesia's geographical location, solar energy appears to be the dominant green energy source (ideally in the future). Solar energy may be harnessed in various methods, the most popular being photovoltaic panels. The main benefit of PV is its independence from other power sources [37]. Under focused solar illumination, the highest conversion rate is around 44% of a PV's (or potential's) total [38], but it is much lower. It is computed as follows in [39]:

$$P_{PV} = S_{PV} \cdot Y_{PV} \cdot \left(\frac{(I_T)}{(I_S)}\right)\left(1 + \alpha_P(T_C - T_{C,S})\right) \quad (1)$$

where: $\boldsymbol{Y_{PV}}$ is the rated power output of all of the PV panels that have been installed (kW), $\boldsymbol{I_T}$ is the amount of solar light that is absorbed by the installation surface (kW/$m^2$), and $\boldsymbol{I_T}$ is radiation to which the panel is subjected for testing and rating (1.0 kW/$m^2$). Moreover, $\boldsymbol{T_C}$ is the ideal temperature for photovoltaic cells, $\boldsymbol{T_{C,S}}$ is the temperature at which a conventional panel test is conducted ($25^0$C), and $\boldsymbol{\alpha_P}$ is the panel's temperature coefficient factor in percentage degrees Celsius. The installation site's radiation data is necessary to estimate the PV output power using Equation (1). NASA's surface meteorology and solar energy databases provide Malang's monthly average global horizontal radiation (GHI) and clearness index (Figure 9). GHI is the total amount of solar energy released on a horizontal plane because flat panels are not nearly as horizontal as they appear to be. Manufacturers provide temperature-specific PV specifications. That means the power output of a solar cell is reduced when its surface temperature rises.

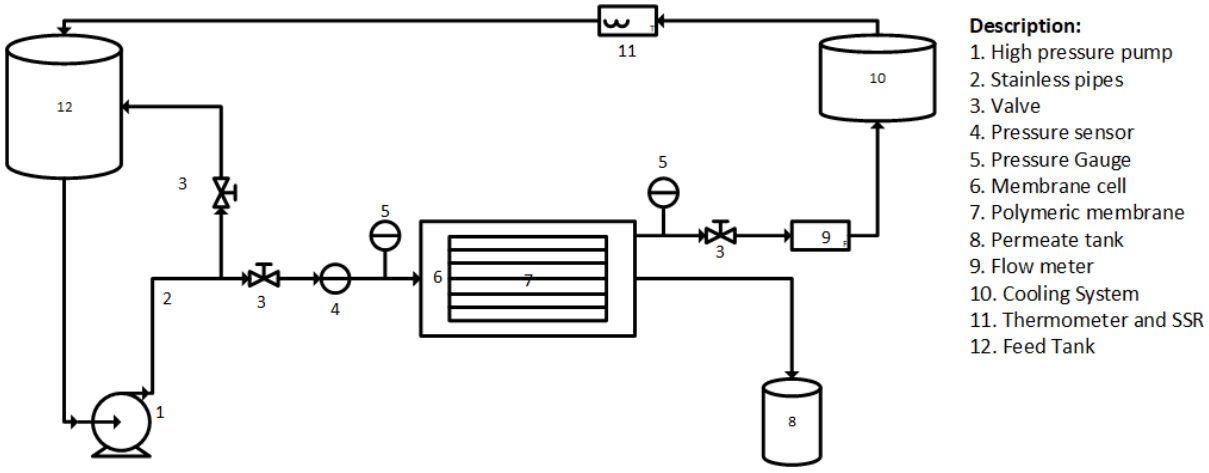


**Fig. 7. An example of an osmosis filtering structure.**

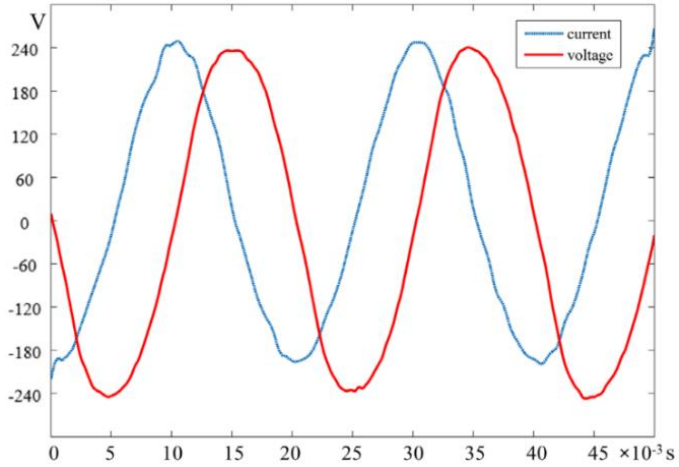


**Fig. 8. Purification system voltage and current measurements.**

The temperature coefficient (%/$^0$C) is more helpful in predicting Indonesia's hot climate and should be considered. The Malang hourly temperature is examined in this piece, and the electricity provided by the PV panels is altered.

### *2.4 Wind Energy*

Wind energy is very changeable in time and place. Technically, higher elevation lands and regions remote from surface plants or building shelters are windier—the wind speed changes at a specific spot every day. However, short-term patterns in wind velocity can be predicted. Although not exact, this estimate can help make wind turbine decisions. Wind turbines can be taller than 10 meters, however these measurements were taken at 10 meters. According to this formula, the wind speed at the height of a wind turbine may be calculated [39]:

$$\frac{V_{Turbine}}{V} = \frac{In\left(\frac{Z_{Turbine}}{Z_0}\right)}{In\left(\frac{Z_{anm}}{Z_0}\right)} \quad (2)$$

where: $\boldsymbol{V_{Turbine}}$ and $\boldsymbol{V}$ are wind velocity at wind turbine height and anemometer height (10 m). $\boldsymbol{Z_{Turbine}}$, $\boldsymbol{Z_{anm}}$, and $\boldsymbol{Z_0}$ are the height of the turbine (m), height of anemometer (m), and the surface roughness length (m), respectively. For different surfaces, the value of surface roughness length is different. For example, surface roughness of 0.10 m is assumed for the installation location, making it suitable for flat regions with minimal trees. Location-specific wind regimes are typically discovered using the two-parameter Weibull distribution, cumulative distribution function (CDF), and density of probabilities [40]:

$$f(V) = \frac{k}{c}\left(\frac{V}{c}\right)^{\cdot k-1} \exp\left(\left(-\frac{V}{c}\right)^{k}\right), \quad (3)$$

$$F(V) = 1 - exp\left(\left(-\frac{V}{c}\right)^{k}\right) \quad (4)$$

where: $\boldsymbol{c}$ is the Weibull scale (m/s), and $\boldsymbol{k}$ is the Weibull shape factor. Combining these formulae yields the average wind velocity as [39]:

$$\bar{V} = c\Gamma\left(\frac{1}{k} + 1\right) \quad (5)$$

The average wind speed at the installation site is seen in Figure 10.However, when operating under a particular wind velocity situation, varied output performances can be attained depending on each wind turbine [41]. The output power of a wind turbine is [39]:

$$P_{Wind} = \frac{1}{2}\tau\rho C_p A \sum_{1}^{j} f_v v^3 \quad (6)$$

where: The wind velocity distribution is denoted by $f_v$, while the wind velocity is denoted by v. A wind turbine's performance may be improved by paying attention to the power curve of each turbine. Figure 11 shows the turbine's power output as a function of wind speed. The optimal wind turbine for a given site has a power curve that matches the average wind velocity.

### 2.5 Generator

Green energy sources may not be totally reliable in a standalone desalination plant. During extended periods of gloomy weather or on days with little wind, the generated electricity may be insufficient. In a hybrid energy system, a generator powered by internal combustion can compensate for this fraction of fossil fuel energy. This article examines a 0–100 kW diesel-powered generator with internal combustion. This generator's yearly output energy (kWh) is [39]:

$$E_{gen} = \frac{\eta_{gen} m_{fuel} LHV_{fuel}}{3.6} \quad (7)$$

where: The efficiency of the generator is denoted by $\eta_{gen}$, $m_{fuel}$ is the annual use of fossil fuels (kg/year), and $LHV_{fuel}$ is the lower heating value of the fuel (MJ/kg). As a result of changes in Indonesia's subsidies, the price of diesel in Indonesia now stands at 0.36 $/liter, although this is expected to climb. The generator can be implemented in two ways: load following or cycle charging. When renewable energy sources are not enough, load following uses a generator to satisfy system demand. However, the generator runs at full power to fulfill demand and charge the batteries. Load following is optimum when the system has limited renewable energy sources. This program modeled and contrasted both techniques.

### 2.6 Battery

The variance of the generated energy throughout the day, night, and windy hours necessitates a battery bank [42]. Therefore, the battery can store low-demand DC and supply it to the system when needed. Beyond the price, it is critical to assess each battery's lifespan, capacity, and voltage. The most familiar green power batteries are lead-acid batteries, which have a low cost per kilowatt-hour. A lower discharge rate and higher performance in both hot and cold climes are the advantages of lead-acid batteries. The longevity of a battery depends on two factors: the number of charge cycles and the standard lifespan (independent of charge and discharge). Depending on the type of battery and the number of cycles, one of these parameters will determine the battery's lifespan. A thorough evaluation of battery life can help us determine whether the use of a battery bank is economical. In this software, computes the number of charges and discharges and then compares the data with the battery's lifespan to determine the battery's cost and its longevity [39].

$$Battery\ life = Min\left[\frac{N_{batt}\, Q_{lifetime}}{Q_{thrpt}}, R_{batt,f}\right] \quad (8)$$

where: The number of batteries that are charged during a single charge cycle is denoted as $N_{batt}$, $Q_{thrpt}$ is the annual storage capacity, while $Q_{lifetime}$ is the capacity of each battery during its whole life. To limit discharge cycles' negative impacts and prevent complete discharge damage to the battery cells, the model avoids discharge levels below 30%. During the charging ($\eta_{ch}$) and discharging process ($\eta_{dch}$), the efficiency is equal to [39].

$$\eta_{ch}, \eta_{dch} = \sqrt{\eta_{rt}} \quad (9)$$

The efficiency of a lead-based battery is fixed at 80 percent for a round trip.

### 2.7 Converter

The generators of a hybrid green energy system can produce either alternating current or direct current. The power generated by the turbine, photovoltaics, batteries, or generator must be converted to the 50 Hz alternating current required by the RO pumping system. A converter can convert direct current to alternating current or modify the frequency of an alternating current (50 Hz). The output power of the converter is significant—this study tests convertibles ranging in power from 0 to 50kW.

### 2.8 Analysis of the Economic Situation

The cost of the operation includes the cost of the initial investment, the cost of replacement (if necessary), and the cost of operation and maintenance. Table 2 displays the costs of the hybrid system's various components; these prices are based on the system's and each component's 20-year lifespan. Annualized cost is a suitable indicator for comparing different combinations of power generators, and it facilitates a fair comparison between components with low capital cost and high maintenance and those with high capital cost and cheap maintenance. The annualized cost of the hybrid system is as follows [39]:

$$C_a = CRF(i, R_{proj}) C_n \quad (10)$$

where: $R_{proj}$ is project lifespan, and real discount rate percent) denoted as $i$. The net present cost is computed by subtracting all revenue from installation and performance costs over the component's lifetime. The present value of an annuity is calculated using the capital recovery factor ($CRF$) [39]:

$$CRF(i, N) = \frac{i(1+i)^N}{i(1+i)^N - 1} \quad (11)$$

**Table 2. The prices of different parts of the system**.

| Item | Capital Cost ($) | Operation and Maintenance ($) |
|---|---|---|
| PV | 2,000 | 321/yr |
| Turbine (windmill) | 29,000/unit | 1,000/unit |
| Generator diesel | 430/kilowatt | 0.03/60 minutes |
| Battery | 1,229 | 420/yr |
| Converter | 308 | 308 |
| Fuel price | 0.36/liter | |

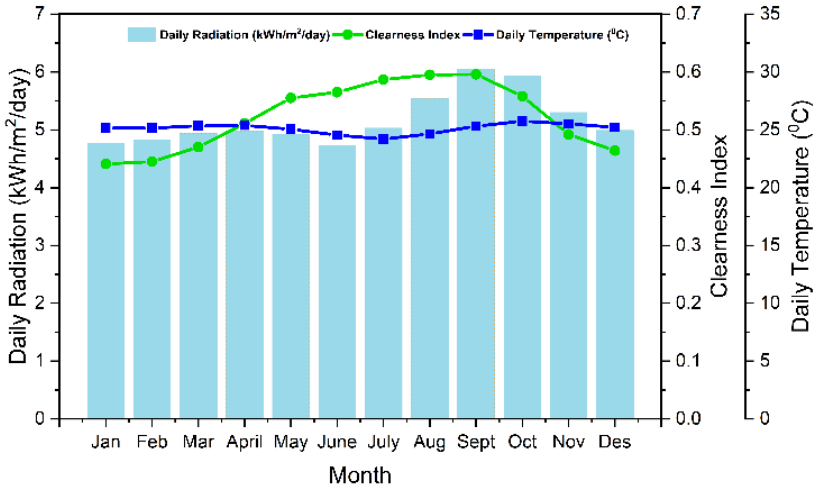


**Fig. 9. The GHI, the temperature, and the clearness index in Tambakrejo every single day.**

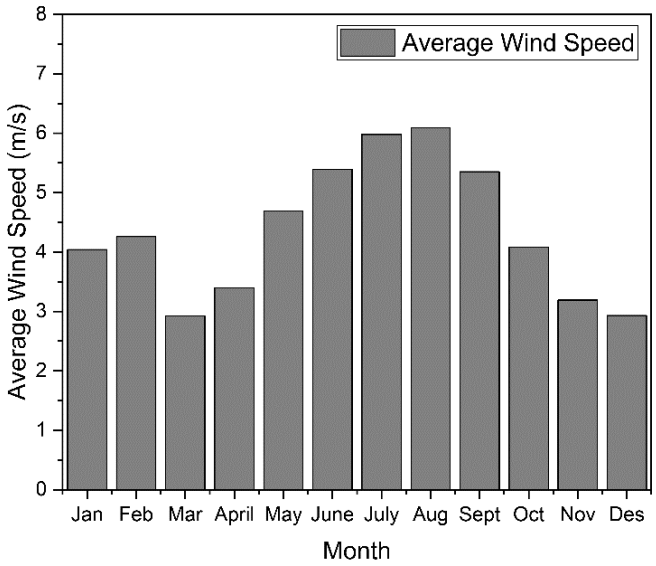


**Fig. 10. Average wind velocity in Tambakrejo.**

## 3. RESULTS AND DISCUSSIONS

Homer utilizes modeling, optimization, and sensitivity analysis to determine the most efficient, effective, and optimal mix of power systems. From the inputted data, estimates of system size/capacity, lifecycle cost, and greenhouse gas emissions will be generated as output. When the coordinates of the HES implementation are entered, data such as wind speed, solar radiation, and other input data are received automatically.

End-user energy policies and renewable energy possibilities can influence RO purification plants using hybrid energy systems. The simulation and comparison of off-grid hybrid systems with possible photovoltaic, wind turbine, battery, and diesel generator combinations. There are two models: those with and without a diesel generator. The advantages of both groups will be discussed in detail later. For example, a power user such as RO may experience peak demand at certain times of the day or month.

For this reason, designing a hybrid energy system may result in an undesirable costly system that is rarely used. To decrease the influence of short-term RO peaks on simulation outcomes, all models incorporate a 5% power capacity shortfall. For example, an Astronergy CHSM6612P/HV-335 polycrystalline panel with 17.1 percent module efficiency and 0.408 percent/C temperature coefficient was used for simulation. A Hengfeng HF12.5–30 kW wind turbine with 12.5-meter diameter blades and an 18-m height will be used. The turbine's lowest starting wind speed is three m/s, and its maximum output is 35 kW. The Trojan SAGM 12205 with 205 Ah big capacity 12 V battery is used in the battery bank. The battery bank size will be determined when each design and simulation is completed. All suggested hybrid systems use the same battery, PV, and wind turbine types.

### *3.1 Generator-Hybrid Systems*

Access to clean drinking water cannot be overstated in its importance. When a hybrid renewable energy system experiences a short-term or even long-term loss of power, it might make water purification risky; a generator can alleviate this problem and reduce the hybrid renewable energy system's potential risk. When it comes to the early hybrid systems, renewable energy sources like wind and solar are combined with generators.

### 3.2 RO using a Generator, Wind, Photovoltaic (PV), and Battery Power

The generator, turbine, solar panels, and batteries were all part of this hybrid system. In order to get the most out of the generator, use below 1 liter of fuel each day and its extreme load of 3.39 kilowatts. As a result of the action, the generator kicks in when the RO plant requires more energy than is provided by renewable sources. When wind and solar power are more than they need for energy, the controller merely charges the battery. An electric vehicle with a 10-year battery bank and seven batteries, for example, is available. Eighty-three percent of the system's useable energy will come from renewable sources thanks to the hybrid system's 30 kW turbine(windmill) and 12 photovoltaic panels with a combined 4.22 kW. An additional $68,139 in capital costs adds up to $98,092 for this hybrid RO plant. It will cost $0.275 ($1.74 per m3 of fresh water) for each kWh of power generated throughout the project's 20-year lifespan.

### 3.3 RO with a Hybrid Energy Source (generator / photovoltaic / battery)

Hybrid solar battery-generator systems are the most cost-effective option compared to other systems. They have a total capital cost of $20,364 and a total cost of $148,875. This hybrid system costs $0.284 per kilowatt-hour and uses a load-following control system that requires 12,205 Ah batteries with a 6.7-year lifetime. Aside from the 37 PV panels, an electric generator provides the remaining 20.9 percent of this RO system's energy demands.

HRES will cover an area of 110.3 square meters and cost $6,800 to install. Additionally, HRES will be permanently implanted. Hybrid systems have higher yearly fuel consumption, with the generator using 3,345 L more gasoline each year.

### 3.4 Generator-Free Hybrid Power (Green Sources)

A hybrid system without a generator is preferable in isolated areas where diesel fuel is challenging to get or in a green purification plant. However, it might last a long time. The following section will look into hybrid systems, including wind turbines, solar panels, and a battery.

### 3.5 Energy RO Hybrid Powered by Photovoltaics and a Battery

PV and a battery-powered hybrid energy system are examined in this model. According to the simulation, this HRES can generate 1 kWh of power for $0.286. While other hybrid systems are more complex and challenging, PV/battery systems are easier to set up. The device requires 43 batteries, each of which must be replaced after only eight years to make things even more complicated. The system must also be completed: a photovoltaic panel with a maximum power of 36 kW must be installed. The initial investment in this hybrid system will be $68,723, and the entire project cost will be roughly $101,686. It will also have to pay for any necessary replacements to make matters worse.

### 3.6 Energy RO Hybrid Powered by Photovoltaics and a Battery

A 60-kW turbine(windmill) and 26 batteries in a storage bank make up the power source in this HES. Compared to the PV/Battery combo, this hybrid system features a smaller battery bank. Compared to the P.V./Battery combo, its battery life is ten years greater. Compared to the prior system, which cost $109,539 initially and $156,799 in the long term, this new system costs less. Replacement and maintenance expenses are also lower than with the prior method. For example, one kWh of electricity will cost $0.458 if all prices are considered.

### 3.7 RO Hybrid with a Turbine, Photovoltaic, and Battery Power

This hybrid energy system comprises a wind turbine, photovoltaic panels, and a battery. Power supply/battery: Without a power source to provide RO on demand, the system relies on a large energy storage facility. The battery bank has shrunk due to the addition of a wind turbine. Batteries have a defined charging period. Therefore, a battery bank with 23 batteries can run the RO plant entirely. Every ten years, the battery bank must be replaced. In addition to two PVs, the hybrid system requires two additional components: A wind turbine of the HF12.5–30 kW kind is also included in this hybrid power system. This system will cost $1004.386 over the next 20 years. This system has a starting price of $63,802. It will cost $0.293 per kilowatt-hour to run the system. Figure 12 shows us how much energy it takes to operate all hybrid systems simultaneously, as shown in the figure.

### 3.8 Gas Emission

It is more environmentally friendly to use renewable energy sources. Climate change is accelerated and exacerbated by emissions of greenhouse gases, including carbon dioxide, carbon monoxide, and unused hydrocarbons. Off-grid electricity from a single generator produces 24,801 kg $CO_2$ per year for this RO plant. By connecting the battery bank to the generator, $CO_2$ emissions are reduced by 15%.

The generator's on-off time is managed, and fuel consumption is reduced by this combination, even if it does not utilize renewable energy. Alternatively, to put it another way, while using the hybrid generator-PV turbine-battery system instead of only the generator, 934 kilograms of $CO_2$ per year are saved. Generator/PV/Battery emits 1,121 kg/year of gas, increasing 20%. Turbines reduce the need to operate the generator at night when the PV panels are not producing electricity. Table 3 lists the gases emitted by the various hybrid powertrain configurations. No emissions are produced by batteries or other solid components for this data.

## 4. CONCLUSION

Hybrid systems combine a range of green energy sources with meeting the end user's needs. The low oil price in Indonesia makes it uneconomical to use renewable energy, although HRES is more practicable in

remote areas with little or no grid connectivity. Off-grid HRES for RO purification plants in Indonesia were studied in this article. Malang, Indonesia, a stand-alone RO purification plant, received daily power from the specified energy infrastructure. For this research's purposes, the daily freshwater demands of a small town were determined, followed by the energy requirements for purification in a RO plant. Solar energy potential, clarity index, wind velocity, and fuel price were all included in the model. Homer Pro was used to simulate all possible PV/wind/DG/battery combinations and found the most cost-effective alternative.

Indonesia's high solar index was the reason for the experiment's results. The most cost-effective off-grid hybrid energy system has 12,205 Ah batteries and 12,5 kW PV panels with a 335 W output each. Adding a 4.3kW generator to this unit may meet all RO requirements. Annual $CO_2$ emissions are 8,700 kg, and the cost per kilowatt-hour (kWh) is $0.275. However, according to computer models, a comprehensive renewable energy system combining PV and wind may be achieved. Turbine/battery hybrids are also an option. Even though HRES costs $0.37 per kWh, it is less polluting and needs less upkeep. To summarize, energy policy and available technology significantly impact the most effective hybrid purifying system.

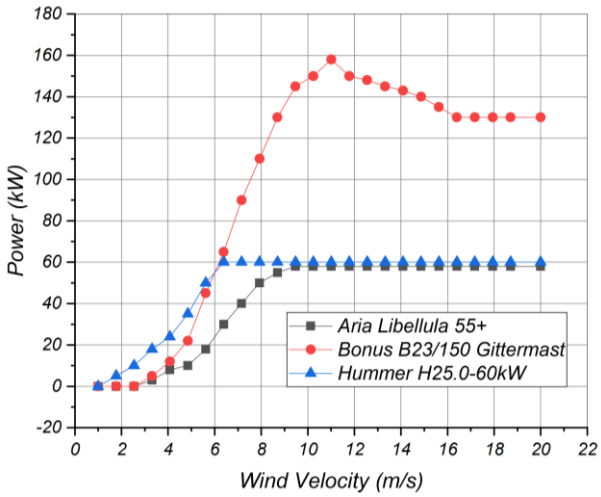


**Fig. 11. A comparison of the power curves of three distinct wind turbines.**

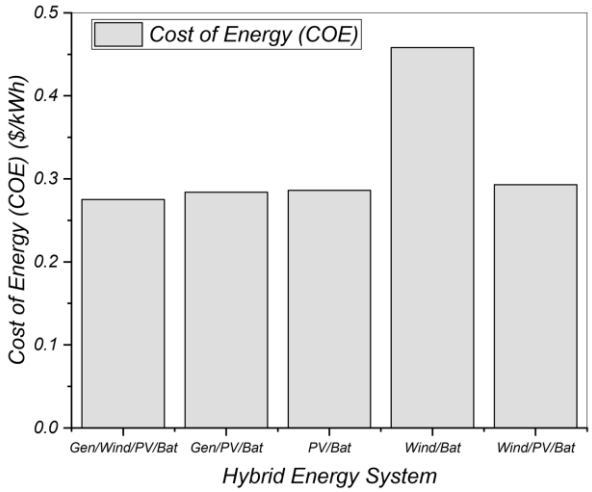


**Fig. 12. Cost of energy for various hybrid energy system configurations**.

**Table 3. The quantity of gas emitted by each hybrid system.**

| Emission | DG | DG/PV/Wind/Bat | DG/PV/Bat | DG/Wind/Bat |
|---|---|---|---|---|
| Carbon monoxide | 165 | 4.89 | 6.56 | 22.3 |
| CxHy | 5.82 | 0.207 | 0.258 | 0.52 |
| $SO_2$ | 56.8 | 2.19 | 2.64 | 8.55 |

Abbreviation: DG = Diesel Generator

## REFERENCES


[1] Abdelshafy A.M., Hassan H., and Jurasz J. 2018. Optimal design of a grid-connected desalination plant powered by renewable energy resources using a hybrid PSO–GWO approach. *Energy Conversion and Management* 173: 331–347.

[2] Al-Obeidani S.K.S., Al-Hinai H., Goosen M.F.A., Sablani S., Taniguchi Y., and Okamura H., 2008. Chemical cleaning of oil contaminated polyethylene hollow fiber microfiltration membranes. *Journal of Membrane Science* 307(2): 299-308.

[3] Ali A., Tufa R.A., Macedonio F., Curcio E., and Drioli E., 2018. Membrane technology in renewable-energy-driven desalination. *Renewable and Sustainable Energy Reviews* 81:1–21.

[4] Ali Z., Sunbul Y.A., Pacheco F., Ogieglo W., Wang Y., Genduso G., and Pinnau I., 2019. Defect-free highly selective polyamide thin-film composite membranes for desalination and boron removal', *Journal of Membrane Science* 578: 85–94.

[5] Burton T., Nick J., Davis S., and Ervin B., 2011. *Wind Energy Handbook*. West Sussex, U.K.: John Wiley & Sons.

[6] Delgado-Torres A.M., Lourdes G., Baltasar P., Juan A., and Gustavo M., 2019. Water desalination by solar-powered RO systems. *Current Trends and Future Developments on (Bio-) Membranes*, 45–84.

[7] Dong Y. Ma L., Tang C.Y., Yang F., Quan X., Jassby D., Zaworotko M.J., and Guiver M.D., 2018. Stable superhydrophobic ceramic-based carbon nanotube composite desalination membranes. *Nano Letters* 18(9): 5514–5521.

[8] Duong H.C., Chivas A.R., Nelemans B., Duke M., Gray S., Cath T.Y., and Nghiem L.D., 2015. Treatment of RO brine from CSG produced water by spiral-wound air gap membrane distillation—A pilot study. *Desalination* 366: 121–129.

[9] Energy, H. (2016) 'Homer pro version 3.7 user manual', HOMER Energy: Boulder, CO, USA, 7.

[10] Fathima A.H. and K. Palanisamy. 2015. Optimization in microgrids with hybrid energy systems–A review. *Renewable and Sustainable Energy Reviews* 45: 431–446.

[11] Funk A. and B.D. William. 2011. Embedded energy in water studies study 3: End-use water demand profiles. California Public Utilities Commission Energy Division, California Institute for Energy and Environment, *CALMAC Study ID CPU0052*.

[12] Greenlee L.F., Desmond F., Lawler B.D.F., Benoit M., and Philippe M., 2009. Reverse osmosis desalination: water sources, technology, and today's challenges. *Water Research* 43(9): 2317–2348.

[13] Gude V.G., 2011. Energy consumption and recovery in reverse osmosis. *Desalination and Water Treatment* 36(1–3): 239–260.

[14] Gude V.G., 2015. Energy storage for desalination processes powered by renewable energy and waste heat sources. *Applied Energy* 137: 877–898.

[15] Hofste R.W., Samantha K., Sara W., Edwin H.S., Marc F.P.B., Marijn J.M., Kuijper M.F.S., Rens V.B., Yoshihide W., and Sandra G.R., 2019. *Aqueduct 3.0: Updated decision-relevant global water risk indicators*. World Resources Institute: Washington, DC, USA.

[16] Homer (2022) 'Homer Pro Software'. Boulder, CO, USA.

[17] Hoseini H. and R. Mehdipour. 2020. Performance evaluation of hybrid solar chimneys for freshwater production. *Environmental Progress & Sustainable Energy* 39(1): 13276.

[18] Hosseinalizadeh, R., Hamed S., Mohsen S.A., and Peyman T., 2016, Economic sizing of a hybrid (PV–WT–FC) renewable energy system (HRES) for stand-alone usages by an optimization-simulation model: Case study of Iran. *Renewable and Sustainable Energy Reviews* 54: 139–150.

[19] Kaldellis, J. K. (2010) Stand-alone and hybrid wind energy systems: technology, energy storage and applications. Elsevier.

[20] Khare V., Nema S., and Baredar P., 2016. Solar–wind hybrid renewable energy system: A review. *Renewable and Sustainable Energy Reviews* 58: 23–33.

[21] Kosai S., 2019. Dynamic vulnerability in stand-alone hybrid renewable energy system. *Energy Conversion and Management* 180: 258–268.

[22] Ma Q. and H. Lu. 2011. Wind energy technologies integrated with desalination systems: Review and state-of-the-art. *Desalination* 277(1–3): 274–280.

[23] Malek P., Ortiz J.M., and Schulte-Herbrüggen H.M.A., 2016. Decentralized desalination of brackish water using an electrodialysis system directly powered by wind energy. *Desalination* 377: 54–64.

[24] Maleki A., 2018. Design and optimization of autonomous solar-wind-reverse osmosis desalination systems coupling battery and hydrogen energy storage by an improved bee algorithm. *Desalination* 435: 221–234.

[25] Manchanda H. and M. Kumar. 2018. Study of water desalination techniques and a review on active solar distillation methods. *Environmental Progress & Sustainable Energy* 37(1): 444–464.

[26] Manju S. and N. Sagar. 2017. Renewable energy integrated desalination: A sustainable solution to overcome future freshwater scarcity in India. *Renewable and Sustainable Energy Reviews* 73: 594–609.

[27] Martínez-Conesa E.J., Ortiz-Martinez V.M., Salar-Garcia M.J., De Los Rios A.P., Hernandez-Fernandez F.J., Lozano L.J., and Godinez C., 2017. A Box–Behnken design-based model for predicting power performance in microbial fuel cells using wastewater. *Chemical Engineering Communications* 204(1): 97–104.

[28] Mehrpooya M., Ghorbani B., and Hosseini S.S., 2018. Thermodynamic and economic evaluation of a novel concentrated solar power system integrated with absorption refrigeration and desalination

cycles. *Energy Conversion and Management* 175: 337–356.

[29] Nema P., Nema R.K., and Rangnekar S., 2009. A current and future state of art development of hybrid energy system using wind and PV-solar: A review. *Renewable and Sustainable Energy Reviews* 13(8): 2096–2103.

[30] Ngan M.S. and C.W. Tan. 2012. Assessment of economic viability for P.V./wind/diesel hybrid energy system in southern Peninsular Malaysia. *Renewable and Sustainable Energy Reviews* 16(1): 634–647.

[31] Padrón I. Deivis A., Marichal G.N., and José A.R. 2019. Assessment of hybrid renewable energy systems to supplied energy to autonomous desalination systems in two islands of the Canary Archipelago. *Renewable and Sustainable Energy Reviews* 101: 221–230.

[32] Parida B., Iniyan S., and Goic R., 2011. A review of solar photovoltaic technologies. *Renewable and Sustainable Energy Reviews* 15(3): 1625–1636.

[33] Politano A., Pietro A., Gianluca D.P., Vanna S., Anna C., Sudip C., Hassan A.A., and Efrem C., 2017. Photothermal membrane distillation for seawater desalination. *Advanced Materials* 29(2): 1603504.

[34] Kalankesh R.L., Rodríguez-Couto S., and Zazouli M.A., 2019. Desalination and power generation of caspian sea by applying new designed microbial desalination cells in batch operation mode. *Environmental Progress & Sustainable Energy* 38(5): 13205.

[35] Rinne H., 2008. *The Weibull Distribution: a Handbook.* New York, USA: Chapman and Hall/CRC.

[36] Schaller R.D. and V.I. Klimov. 2004. High efficiency carrier multiplication in PbSe nanocrystals: implications for solar energy conversion. *Physical Review Letters APS* 92(18): 186601.

[37] Singh R., 2010. Design of dual-purpose membrane desalination systems. *Environmental Progress & Sustainable Energy* 29(3): 349–357.

[38] Sinha S. and S.S. Chandel. 2014. Review of software tools for hybrid renewable energy systems. *Renewable and Sustainable Energy Reviews* 32: 192–205.

[39] Surwade S.P., Sergei N.S., Ivan V.V., Raymond R. U., Gabriel M.V., Sheng D., and Shannon M.M., 2015. Water desalination using nanoporous single-layer graphene. *Nature Nanotechnology* 10(5): 459–464.

[40] Wang H., 2018. Low-energy desalination. *Nature Nanotechnology* 13(4): 273–274.

[41] Yilanci A., Dincer I. and Ozturk H.K., 2009. A review on solar hydrogen/fuel cell hybrid energy systems for stationary applications. *Progress in Energy and Combustion Science* 35(3): 231–244.

[42] Zhang G., Baojia W., Akbar M., and Weiping Z., 2018. Simulated annealing-chaotic search algorithm-based optimization of reverse osmosis hybrid desalination system driven by wind and solar energies. *Solar Energy* 173: 964–975.

[43] Zhang W., Maleki A., Rosen M.A., and Liu J., 2019. Sizing a stand-alone solar-wind-hydrogen energy system using weather forecasting and a hybrid search optimization algorithm. *Energy Conversion and Management*180: 609–621.